RSC Advances

PAPER

View Article Online
View Journal | View Issue

Cite this: *RSC Adv.*, 2022, **12**, 23346

Photocurable acrylate epoxy/ZnO–Ag nanocomposite coating: fabrication, mechanical and antibacterial properties

Thien Vuong Nguyen,*[ab] Truc Vy Do,[ab] Thanh Dung Ngo,[ab] Tuan Anh Nguyen,[a] Le Trong Lu,[ab] Quoc Trung Vu,[c] Lan Pham Thi[a] and Dai Lam Tran*[ab]

In this study, a UV-curable acrylate epoxy nanocomposite coating has been prepared by incorporation of ZnO–Ag hybrid nanoparticles. For this purpose, firstly ZnO–Ag hybrid nanoparticles were fabricated by a seed-mediated growth method. Then, these ZnO–Ag hybrid nanoparticles (2 wt%) were added into the UV-curable acrylate resin matrices. The photocuring process of nanocomposite was evaluated by various factors, such as the conversion of acrylate double bonds, pendulum hardness and gel fraction. Under the 4.8 s UV-exposure time for full crosslinking, the obtained data indicated that incorporation of ZnO–Ag nanohybrids into the coating matrix changed the crosslinking process of coating significantly. A mechanical teat indicated that the presence of nanohybrids in photocurable coating matrix enhanced its abrasion resistance from 98.7 to 131.6 L per mil (33.3%). The antibacterial test against *E. coli* over 7 h indicated that *E. coli* bacteria were killed totally by nanocomposite coating, whereas it was 2.6×10^4 CFU mL^{-1} for the neat coating without nanoparticles.

Received 8th June 2022
Accepted 18th July 2022

DOI: 10.1039/d2ra03546d

rsc.li/rsc-advances

1. Introduction

Organic coatings have been used widely for protection and decoration of various substrates.[1,2] Regarding the environmental issue, solvent based coatings should be replaced by non-solvent based coatings, such as water-based or photocurable resin coatings.[2–6] The photocuring process exhibits many advantages, such as good transparency, high gloss, good mechanical properties, and high resistance against moisture/chemical/weathering.[4,7] The UV-curable coating refers to the UV-crosslinking polymerization of resins, which consists of some important agents, such as the photoinitiator, and functional monomers/oligomers. The photocurable resin systems have two main systems, such as (i) radical photo-polymerization and (ii) cationic photo-polymerization resin systems. In this regard, their polymerization process undergoes four steps, including photolysis of initiator, initiation, chain propagation and termination.[7]

To fabricate the antibacterial organic coatings, inorganic nanoparticles can be added into the coating matrices.[8] As reported, these main inorganic nanoparticles are nano-TiO_2, nano-ZnO and nano-Ag, which act as antibacterial agents for organic coatings.[8–13] Ag nanoparticles (nano-Ag or AgNPs) have been considered the most used and effective anti-microbial nanoparticles against both *Gram-positive* bacteria and *Gram-negative*. Hybridization of AgNPs with metal oxides is a new approach to enhance the antibacterial effect of AgNPs.[14–17] In this regard, ZnO can be used to support AgNPs for controlling stability and minimizing the toxicity of free silver to human cells.[14] Regarding the antibacterial application of nano-ZnO particles, due to their large band gap (~3.2 eV), they can kill the bacteria only under UV light radiation. In addition, the antibacterial application of nano-ZnO is limited, since nano-ZnO exhibit the low photoenergy conversion efficiency, with low charge separation efficiency and fast recombination of photogenerated charge carriers.[15] In this case, hybridization of nano-ZnO with AgNPs is expected to defeat the large band gap of ZnO.[15] In the hybrid nanostructures, the visible light absorption by surface plasmon resonance (SPR) of AgNPs could induce the electron transfer to nano-ZnO, resulting in charge separation and therefore activated by visible light. Thus, the antibacterial and photocatalytic activities of nano-ZnO are improved significantly by hybridization with AgNPs.[15]

It was reported in literature that various nanofillers could be added into the photo-curable resins.[12,18–22] For the crosslinking of thermoset resin system, the presence of additives can affect to the components of paint formulations.[23–33] Regarding the epoxy nanocomposite, nanofillers could act as a bridge for the interconnected molecules, and thus reduce the free volume and increase the crosslinking density.[24,25] For UV-curable systems,

[a]*Institute for Tropical Technology, VAST, 18 Hoang Quoc Viet, Cau Giay, Hanoi, Vietnam. E-mail: trandailam@gmail.com*

[b]*Graduate University of Science and Technology, VAST, 18 Hoang Quoc Viet, Cau Giay, Hanoi, Vietnam*

[c]*Faculty of Chemistry, Hanoi National University of Education, 136 Xuan Thuy, Cau Giay, Hanoi, Vietnam*

influence of certain additives on their photocrosslinking are reported.[26]

Recently, Nguyen *et al.*[27,28] reported the synthesis and antibacterial activity of ZnO–Ag nanohybrids. The authors found the good antibacterial activity against *Staphylococcus aureus* and *Escherichia coli* bacteria, even at low content (<40 mg mL^{-1}) with the higher inhibition areas. In addition, their antibacterial activity was higher with light irradiation than those in the dark. Incorporation of ZnO–Ag nanohybrids into the organic coatings would provide high antibacterial activity for the coating. This study explores how UV-curable nanocomposite coating can exhibit the antibacterial activity.

2. Materials and methods

2.1. Materials

Silver nitrate, nano-ZnO (<100 nm, Fig. 1), 1-octadecene (ODE, 90%), oleylamine (OLA, 70%), 1-octadecanol (OCD-ol, 99%), ethanol and hexane were provided by Sigma-Aldrich (Singapore).

Bisphenol A glycerolate dimethacrylate (BGDM) and 1,6-hecxanediol diacrylate (HDDA, 80%) used as a diluent were purchased from Sigma-Aldrich; 1-hydroxy-cyclohexyl-phenyl-ketone, Irgacure 184 (I.184) used as a photoinitiator was purchased from CIBA, Germany. Fig. 2 presents the chemical structures of these UV-curable reagents.

2.2. Synthesis of ZnO–Ag hybrid nanoparticles

ZnO–Ag hybrid nanoparticles are synthesized by seed-mediated growth method[29] using as-received nano-ZnO (<100 nm) as the seeds, oleic acid (OLA) as ligand and 1-octadecene (ODE) as solvent/reducing agent for $AgNO_3$ precursors. The details of method for synthesis are reported in our previous work.[17,30] The formation process of ZnO–Ag nanohybrids can be described in Fig. 3. Briefly, the mixture A (10 mg of $AgNO_3$, 6 mL of OLA, 300 mg of ODE and 40 mL of ODE) was prepared and added into a 3-necked flask. The mixture B was prepared by dispersing 100 mg of ZnO in 2 mL of *n*-hexane. Then mixture B was added into mixture A (in the 3-necked flask) under magnetic stirring with the hotplate in presence of heater/nitrogen gas controller. The reaction mixture (A + B) was stirred and kept at room temperature for 30 minutes. Then, the reaction temperature was increased to 80 °C and maintained at this temperature for 30 minutes. In the next stage, the reaction temperature was continuously increased to 200 °C, then refluxed for 60 minutes. During this reaction stage, $AgNO_3$ salt was reduced directly on the nano-ZnO surface to form silver nanocrystals attached to nano-ZnO.

Once the reaction stopped, the mixture system was cooled down to room temperature, then ethanol was added into the product solution to form the agglomeration between the nanoparticles. To collect the nanohybrids, centrifugation at 10 000 rpm was carried out for 5 minutes. Finally, the precipitation of nanohybrids was re-dispersed into the *n*-hexane solvent. Chemical residues were removed by adding fresh *n*-

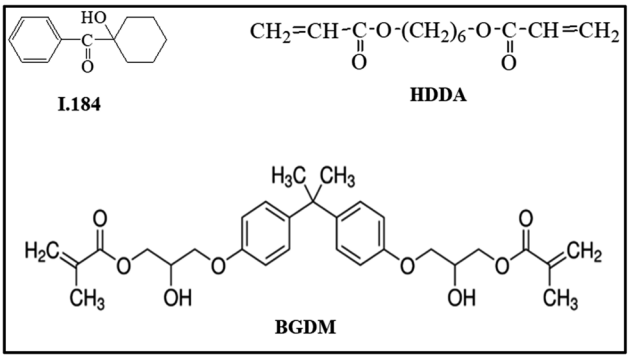

Fig. 2 Chemical formulas of I.184, HDDA and BGDM.

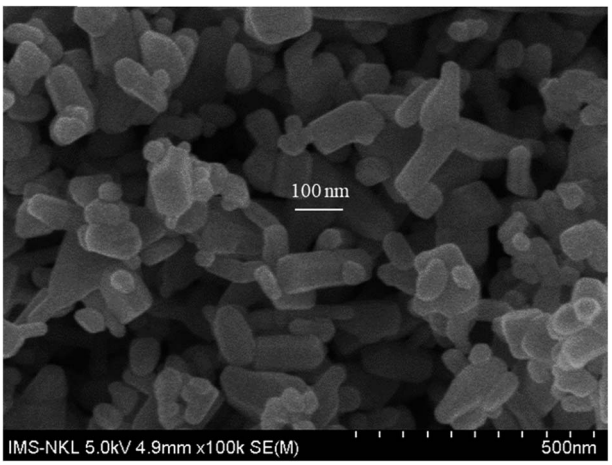

Fig. 1 FE-SEM photographs of as-received nano-ZnO.

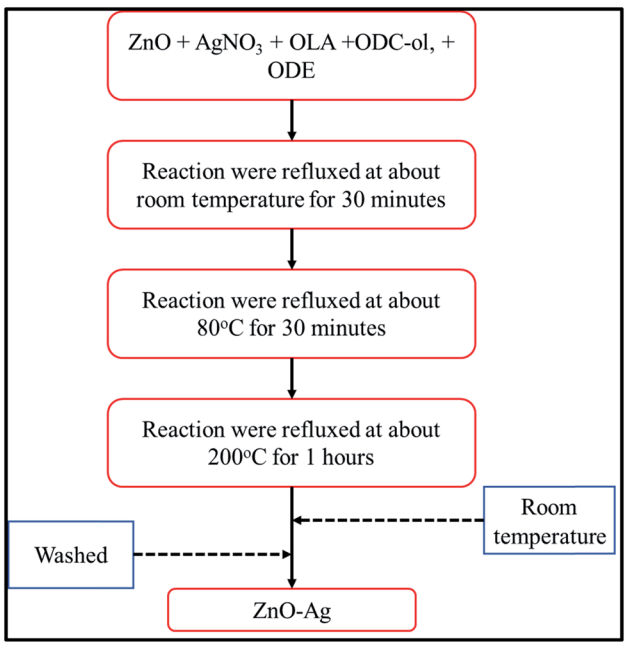

Fig. 3 Scheme for fabrication of ZnO–Ag nanohybrids.

hexane solvent several times in the centrifugation. Final nanohybrids powder was dried naturally at room temperature.

2.3. Fabrication of nanocomposite coating

Firstly, ZnO–Ag nanohybrids were dispersed in HDDA under sonication (25 KHz, 3 hours). Secondly, BGDM and I.184 were added into this mixture with the presence of mechanical stirring (600 rpm for 30 min). The content of nanohybrids was 2% by weight of HDDA and BGDM, whereas the ratio of E284 : HDDA : I.184 was 55 : 45 : 3.

Thirdly, from the as-prepared solution, 25 μm of thick layers were coated on various substrates, such as Kerr pellets (for IR study), Teflon sheets (100 × 100 × 10 mm, for GF and FE-SEM studies), and glass plates (100 × 100 × 2 mm, for pendulum hardness and abrasion resistance tests). Finally, the curing process was carried out on the coated samples by exposure to UV-light using the FUSION UV (Model F300S, USA).

2.4. Characterization of ZnO–Ag nanohybrids

Morphological study of ZnO–Ag nanohybrids and their dispersion into coating matrices has been carried out using Transmission Electron Microscopy (TEM, JEM 1010, JEOL, Japan) and Scanning Electron Microscopes (FESEM-S4800-Hitachi and SEM/EDX-JSM 6510LV-JEOL, Japan). X-ray diffraction (XRD) patterns were obtained by a Siemens D5000 (Bruker, USA), whereas the UV-vis absorption spectra were measured by using CINTRA 40 (GBC Scientific Equipment, USA).

The band gap (E_g) of as-received nano-ZnO and as-synthesized ZnO–Ag nanohybrids was calculated from the UV-vis diffused reflectance spectra (UV-2600, Shimadzu, Japan), using the Tauc method.[31]

2.5. Characterization of UV-cured coatings

To evaluate quantitatively the chemical conversion of acrylate double bonds (AD bonds), FTIR study was used, focusing on the characteristic band at 984 cm^{-1} (=CH stretching) during crosslinking. The details of this method was reported in previous works.[17,30] The gel fraction (GF) of cured coatings was determined by using a Soxhlet (in acetone, for 24 hours), under the standard ASTM D 2765.[30]

To study the mechanical properties of coatings, relative hardness (pendulum hardness) was measured by using pendulum damping tester (ASTM D 4366 standard). Whereas,

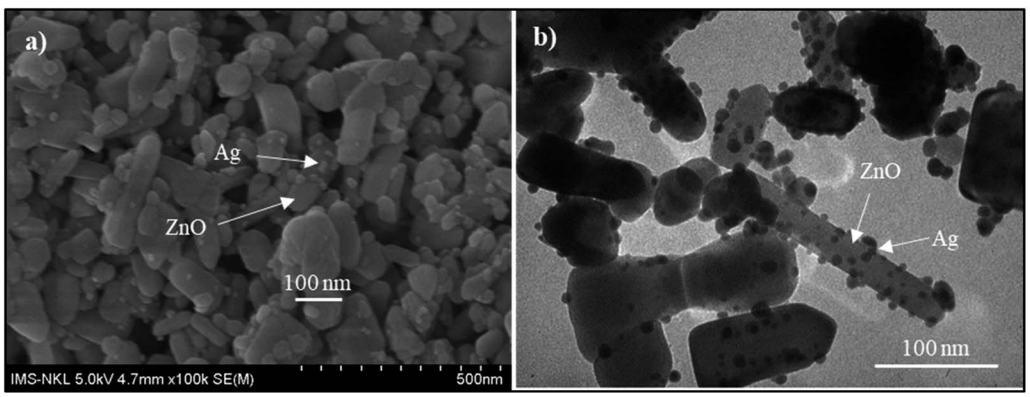

Fig. 4 FE-SEM (a) and TEM (b) photographs of ZnO–Ag nanohybrids.

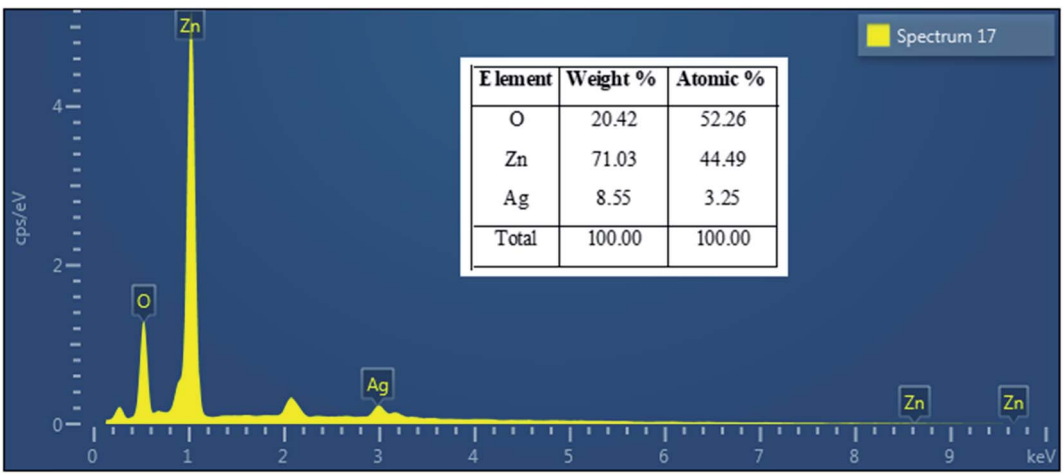

Element	Weight %	Atomic %
O	20.42	52.26
Zn	71.03	44.49
Ag	8.55	3.25
Total	100.00	100.00

Fig. 5 EDX spectra of ZnO–Ag nanohybrids.

abrasion resistance was measured by using the abrasive falling methods (ASTM D968 standard).

2.6. Antibacterial activity test for UV-cured coatings

The antibacterial test of UVAE and UVAE/ZnO–Ag coatings was performed according to the 22196:2007 standard by using *Escherichia coli* strain DH5α (Invitrogen Corp.). Firstly, the *Escherichia coli* (*E. coli*) strain was activated overnight on LB fluid (Luiria Bertani broth) so that the number reached 10^9 CFU mL^{-1}. The bacterial solution after being activated is evenly dripped with the same amount (with a concentration of 3.4×10^5 CFU mL^{-1}) on the surface of the coated glass coupons ($50 \times 50 \times 2$ mm). The glass panels are illuminated with fluorescent lamps usually at the temperature of (35 ± 1) °C. The antibacterial ability of the samples was evaluated through the number of *E. coli* bacteria surviving on the surface of the glass slide before and after 7 h of the experiment.[32,33]

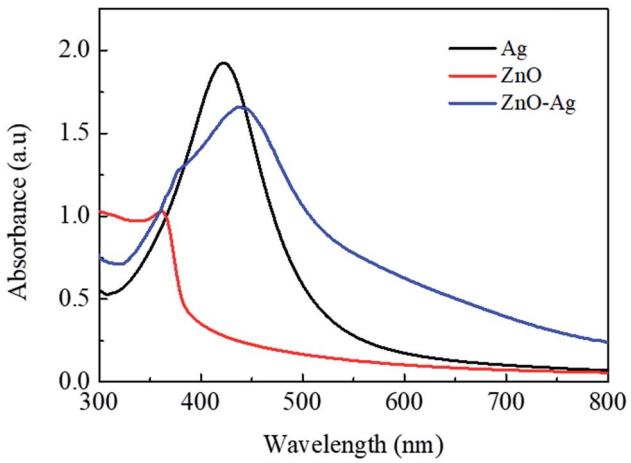

Fig. 6 UV-vis absorption spectra of ZnO–Ag nanohybrids (ZnO–Ag), pure ZnO nanoparticles (ZnO) and pure Ag nanoparticles (Ag).

3. Results and discussion

3.1. Characterization of ZnO–Ag nanohybrids

Fig. 4 presents the FE-SEM and TEM photographs of ZnO–Ag nanohybrids. As shown in Fig. 4, AgNPs present the irregular shape with average size of ~10 nm, which are attached to the as-received nano-ZnO (<100 nm). Energy-dispersive X-ray (EDX) analysis (Fig. 5) shows the content of AgNPs in ZnO–Ag hybrid nanoparticles is ~8.55 wt%.

UV-visible absorption spectra of ZnO–Ag nanohybrids (ZnO–Ag), pure ZnO nanoparticles (ZnO) and pure AgNPs (Ag) were presented in Fig. 6. As can be seen in Fig. 5, the broad absorption peak of the single nano-ZnO is found at 361.8 nm,[34] whereas strong absorption peak of the single AgNPs (localized surface plasmon resonance, LSPR peak) of AgNPs is observed at 423.2 nm. In case of ZnO–Ag nanohybrids, a broad (strong) peak at 440.6 nm and a shoulder (weak) at 362/370 nm are observed. Interestingly, hybridization of nano-ZnO and AgNPs exhibits the red shift of LSPR peak position from 423.2 to 440.6 nm. This result confirms that AgNPs are not only formed/attached to the surface of nano-ZnO, but also hybridized with nano-ZnO. This red shift of LSPR band is coherent with the data reported for Ag/ZnO core–shell composites[35] and other noble metal–metal oxide hybrid nanoparticles.[36] This red shift of LSPR band can be explained by the strong interfacial electronic coupling between neighboring nano-ZnO particles and nano-Ag.[37,38]

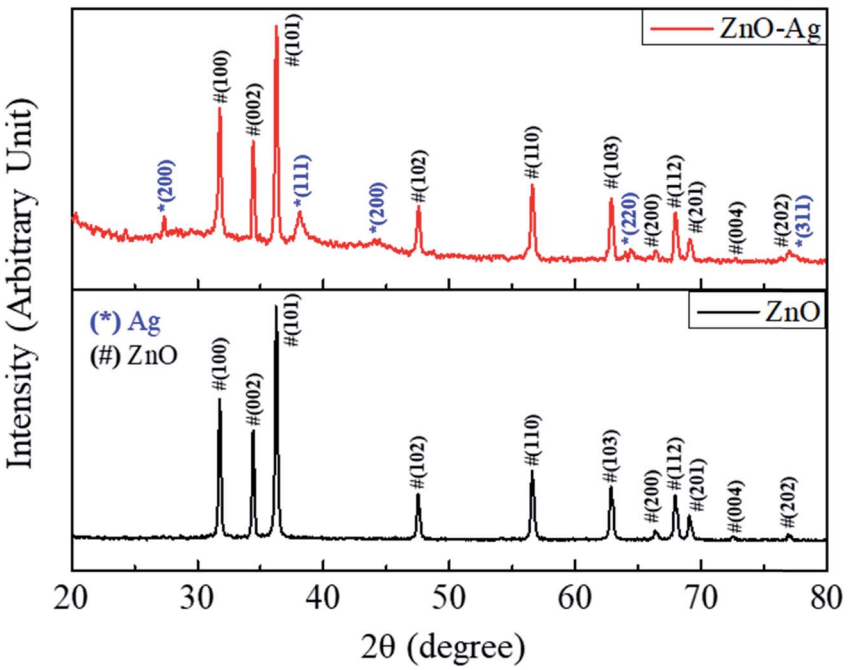

Fig. 7 XRD diffraction diagrams of ZnO–Ag nanohybrids (ZnO–Ag) and pure ZnO nanoparticles (ZnO).

The structural characteristics of nanoparticles were then studied by XRD method. Fig. 7 shows the XRD diffraction patterns of ZnO–Ag nanohybrids and as-received nano-ZnO. As shown in Fig. 7, the hexagonal crystal structure of ZnO are observed by their characteristic planes of (100), (002), (101), (102), (110), (103), (112) and (201) (based on the reference of JCPDS no. 36-1451). These similar characteristic planes are found in the XRD pattern of ZnO–Ag nanohybrid, along with the presence of AgNPs in face-centered cubic structure. As shown in Fig. 5, the face-centered cubic structure of AgNPs is characterized by lattice planes for (220), (111), (200), (220) and (311) (with the reference of JCPDS no. 04-0783).

Fig. 8 presents the plots of $F(R)^2$ *vs.* photon energy of as-received nano-ZnO and ZnO–Ag nanohybrids. As estimated, the band gap energy (E_g) of ZnO is 3.2 eV. Hybridization with AgNPs reduces the E_g value of ZnO (from 3.2 to 2.6 eV). This finding confirms that Ag particles have been attached to the surface of ZnO particles. This can be explained by the hybridization of Ag with ZnO.

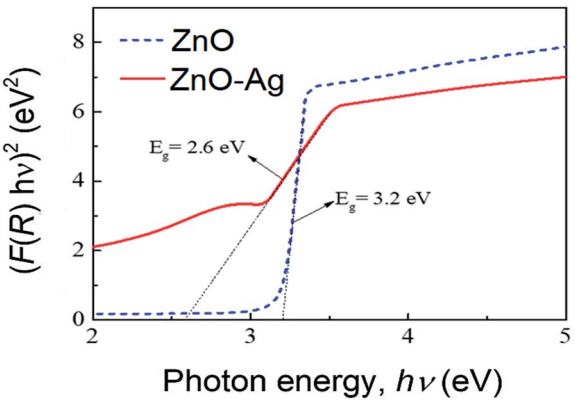

Fig. 8 Plots of $F(R)^2$ *vs.* photon energy, obtained using UV-vis diffuse reflectance spectra, of the as-synthesized materials; pure ZnO and ZnO–Ag nanohybrid.

3.2. Study on crosslinking process of UV-curable nanocomposite coatings

Fig. 9 presents the IR spectra of UV-curable UVAE and UVAE/ZnO–Ag coatings, before and after UV light exposure (4.8 second of irradiated time). As can be seen in Fig. 9, during the curing stage, we observe the reduction of characteristic bands at 1635, 1409, 984 and 810 cm^{-1}, which are attributed to AD bonds of HDDA and BGDM. Among these bands, the intensity of 984 cm^{-1} band reduces the most visible. Thus, we consider this peak as reference for quantitative evaluation of AD bonds' conversion during the crosslinking stage of this coating system. Fig. 10 shows the conversion of AD bonds during the UV-light irradiation for UVAE and UVAE/ZnO–Ag coatings.

As seen in Fig. 10, the AD bonds are converted mainly in the first 0.15 second, then its conversion becomes stable. After 4.8 s of UV-light irradiation, the conversion of the AD bonds reaches to the highest value, *i.e.* 87.24% and 90.39% for the UVAE and UVAE/ZnO–Ag (2 wt%) coatings, respectively. Thus, the

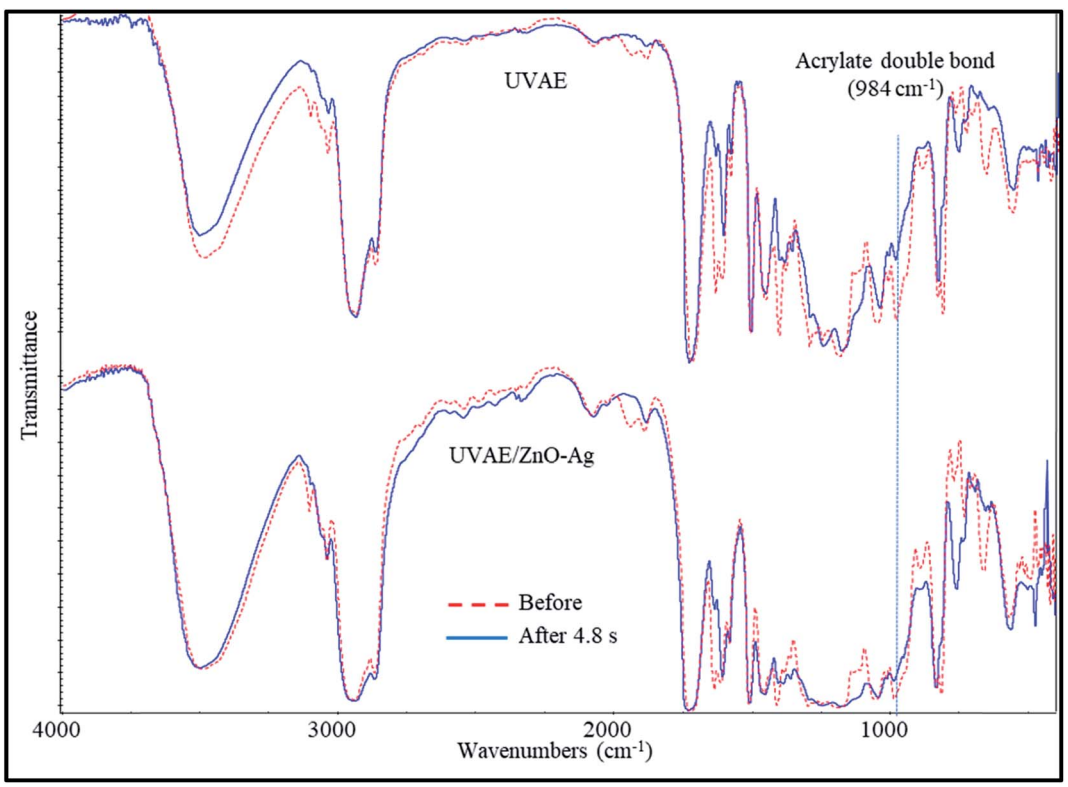

Fig. 9 IR spectra of UV-curable UVAE and UVAE/ZnO–Ag coatings, before and after UV light irradiation.

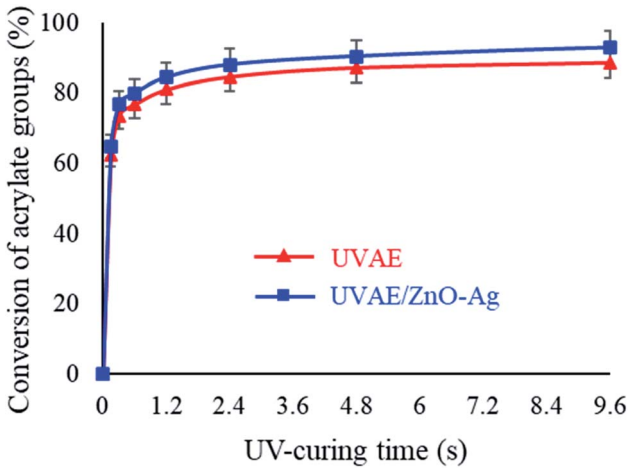

Fig. 10 Conversion of AD bonds during the UV exposure.

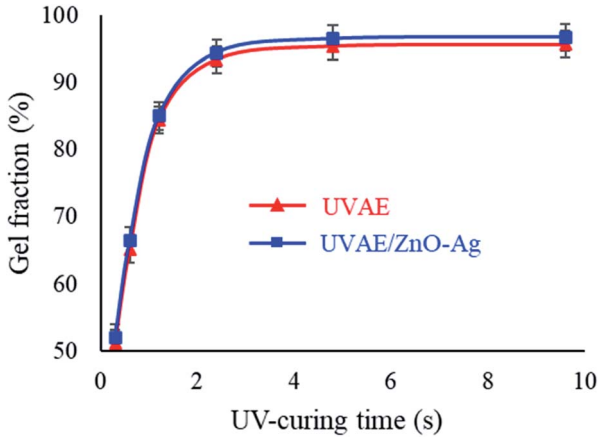

Fig. 11 Evolution of GF for UVAE and UVAE/ZnO–Ag coatings during the curing.

conversion of AD bonds in the UVAE/ZnO–Ag coating is slightly higher than that in the UVAE coating. A possible explanation is that the conversion of the AD bonds could be influenced by photocatalysis of ZnO–Ag nanohybrids. We have also observed

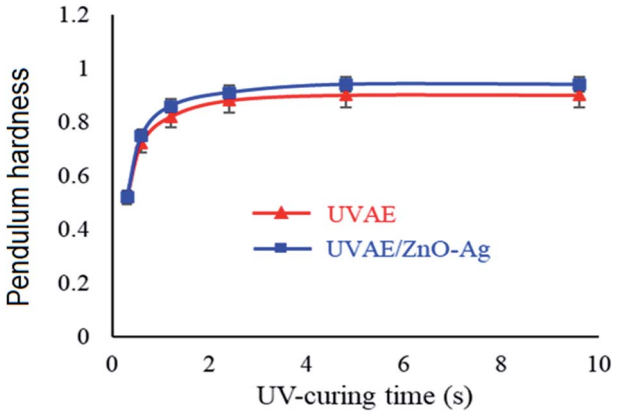

Fig. 13 Variation of coating pendulum hardness during curing process for UVAE and UVAE/ZnO–Ag coatings.

similar effect in case of other photocatalysts like A-TiO_2 and ZnO. Besides, the photocatalytic activity of ZnO–Ag nanohybrids is stronger than single nano-ZnO.[39]

Fig. 11 shows the evolution of GF by the time of curing for the UVAE and UVAE/ZnO–Ag coatings. As shown in Fig. 11, GF of the coatings could be detected after 0.3 second under UV-light irradiation. Then, GF of the coatings increase rapidly for the next 2.4 second, but slowly till 4.8 second. After 4.8 second of exposure, the GF reaches a maximum values, *i.e.* 95.45% and 96.53% for the UVAE and UVAE/ZnO–Ag coatings, respectively. Thus, incorporation of ZnO–Ag nanohybrids into the coating matrix increases on its GF. This finding also can be explained by the photocatalytic enhancement of hybrid particles that promotes the crosslinking reaction. As a comparative study, in the previous work on UV-curable acrylate/Fe_3O_4–Ag nanocomposite,[30] we reported that the presence of Fe_3O_4–Ag hybrid nanoparticles in UV-curable coating matrix did not change its crosslinking process. We also found that loading of nano-TiO_2 (anatase) and nano-ZnO particles (at 2 wt%) to the resin led to an increase in the curing conversion. However, nano-TiO_2 (rutile) particles had no effect on photocrosslinking polymerization (fairly negligible at 2 wt%).[40] For nano-SiO_2, their incorporation into the coating matrix (at 2.5 wt%) increased the

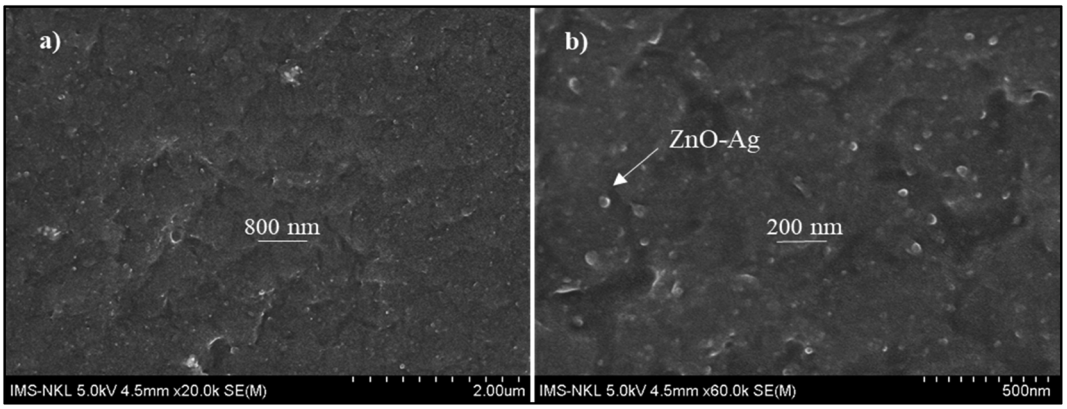

Fig. 12 FE-SEM photographs of UV-cured UVAE/ZnO–Ag in cross-section: (a) ×20 000 and (b) ×60 000.

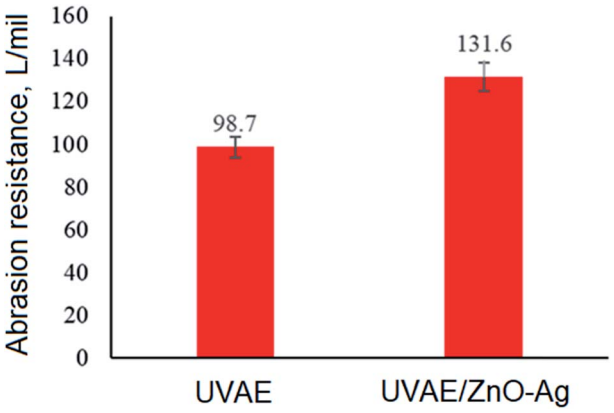

Fig. 14 Values of abrasion resistance for UV-cured UVAE and UVAE/ZnO–Ag coatings.

curing conversion.[41] Thus, the effect of these nanoparticles on the crosslinking process of UV-curable coatings depends on the competition between their roles as UV-absorbents and photocatalysts as well.

3.3. Morphology and mechanical properties of nanocomposite coatings

Fig. 12 presents the cross-sectional images of UVAE/ZnO–Ag coating. As shown in Fig. 12, the coating exhibits a dense structure with homogenous dispersion of nanohybrids in the polymer matrix. This dense structure is expected to increase the hardness of nanocomposite coating, due to both reasons of crosslinking degree and nanofillers. Please note that under UV-light irradiation of the crosslinking stage, the liquid curable resin system was converted into a three dimensional polymer network. In addition, the nanohybrids could also contribute their positive effects as both nanofillers and nano-photocatalysts to the crosslinking process. As photocatalyst,

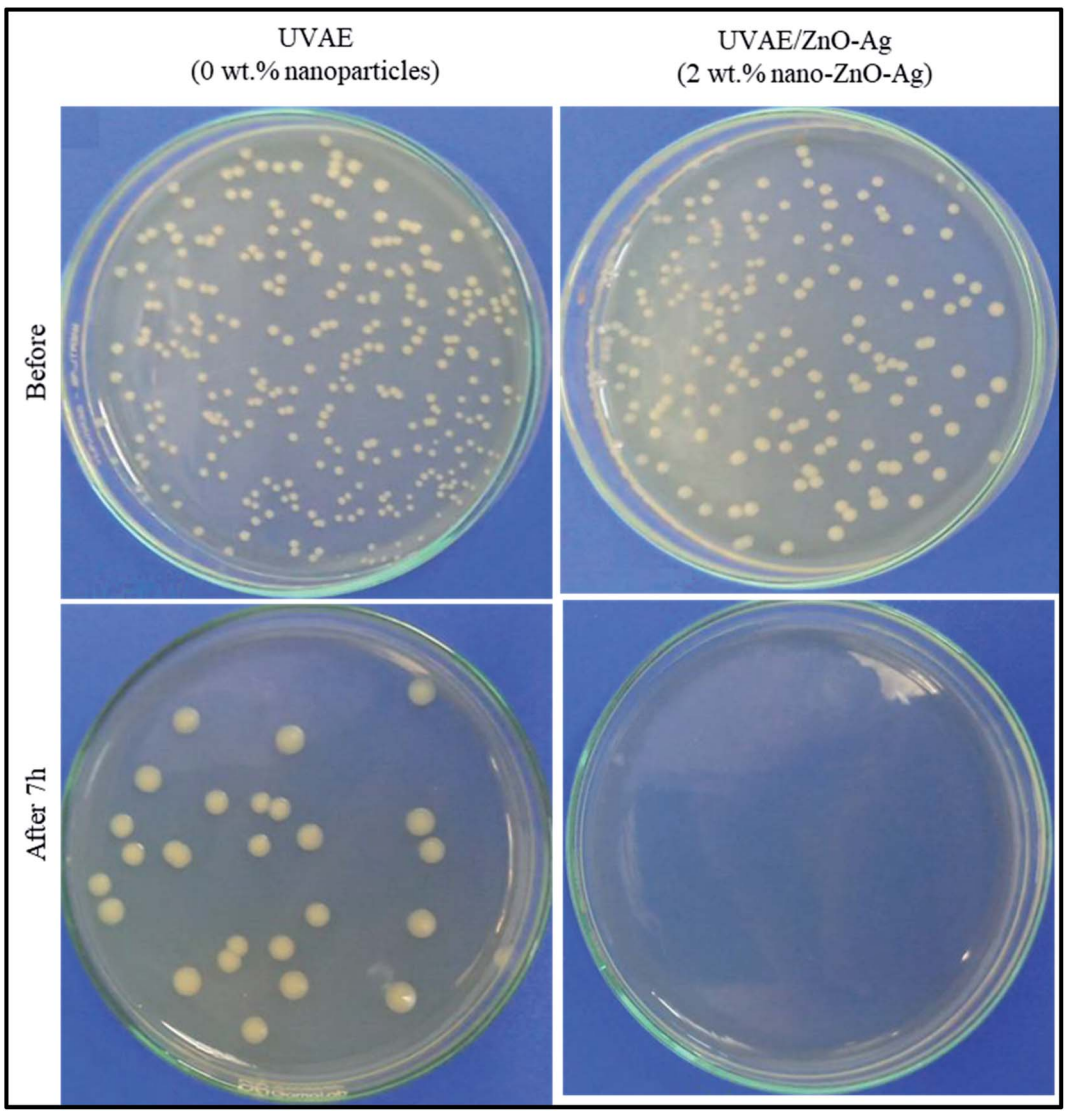

Fig. 15 Photographs of Petri dishes for antibacterial test samples.

Table 1 The number of *E. coli* bacteria surviving on the surface of the glass slide

No	Coating samples	Number of *E. coli* bacteria, CFU mL^{-1}	
		Before	After 7 h
1	UVAE (without nanohybrids)	3.4×10^5	2.6×10^4
2	UVAE/ZnO–Ag (2 wt% nanohybrids)	3.4×10^5	0

hybrid particles may promote the crosslinking reaction at the great depth from the irradiated surface.

Fig. 13 presents the evolution of the pendulum hardness during the curing process for UVAE and UVAE/ZnO–Ag coatings. As shown, the pendulum hardness of coatings increased quickly after the first 1.2 second under UV-light irradiation, till 3.6 second of curing. After 4.8 second, the pendulum hardness reaches a highest values, *i.e.* 0.90 and 0.94 for the UVAE and UVAE/ZnO–Ag, respectively. Thus, as expected, incorporation of ZnO–Ag nanohybrids into the coating matrix increases its pendulum hardness.

Fig. 14 present the values of abrasion resistance for UV-cured UVAE and UVAE/ZnO–Ag coatings. As can be seen from Fig. 14, addition of ZnO–Ag nanohybrids into the polymer matrix increases the abrasion resistance of coating from 98.7 to 131.6 L per mil (33.3%). This finding is coherent with the data from FESEM and pendulum hardness studies.

3.4. Antibacterial activity study of nanocomposite coatings

Fig. 15 and Table 1 present the quantitative data of viable *E. coli* cells before and after 7 h with the presence of UVAE and UVAE–ZnO–Ag coatings. For the coating without nanohybrids (UVAE), the number of *E. coli* viable cells decreases from 3.4×10^5 CFU mL^{-1} to 2.6×10^4 CFU mL^{-1} after 7 h. Whereas, with the presence of nanocomposite coating (UVAE/ZnO–Ag), all viable *E. coli* cells before test (3.4×10^5 CFU mL^{-1}) are killed totally after 7 h. Thus, the nanohybrids provide high antibacterial activity against *E. coli* to the UV-curable acrylate epoxy coating.

The antibacterial activity of ZnO–Ag nanohybrids against different bacteria has been reported recently by Fouladi-Fard *et al.*[42] The authors found their high antibacterial activity against *K. pneumoniae*, *S. typhimurium*, *P. vulgaris*, *S. mitis*, and *S. faecalis* with minimum inhibitory concentration (MIC) values of 50, 12.5, 12.5, 12.5, and 12.45 μg mL^{-1}, respectively. In addition, for ZnO–Ag nanocomposites, Cuadra *et al.*[43] indicated that more than 90% of inoculated bacteria (*S. aureus* and *E. coli*) have been eliminated when the Ag contents of 1 at% was used.

4. Conclusion

ZnO–Ag nanohybrids were successfully prepared by seed-mediated growth method. Data from SEM, TEM, XRD, UV-vis and UV-Vis diffuse reflectance spectra confirmed the hybridization of AgNPs and nano-ZnO with the reduction of E_g from 3.2 eV to 2.6 eV.

Data from the kinetic of UV-curing reaction indicated that adding 2 wt% of hybrid nanoparticles into the coating matrix changed significantly its crosslinking process. FESEM photographs of cross-section for UVAE/ZnO–Ag coating revealed a dense structure with homogenous dispersion of nanohybrids in the polymer matrix.

Data from mechanical studies indicated that incorporation of ZnO–Ag hybrid nanoparticles into the polymer matrix increased not only its abrasion resistance (from 98.7 to 131.6 L per mil), but also its pendulum hardness.

Antimicrobial study indicated that the nanohybrids provide high antibacterial activity against *E. coli* to the UV-curable acrylate epoxy coating. All viable *E. coli* cells before test (at concentration of 3.4×10^5 CFU mL^{-1}) are killed totally after 7 h by presence of UVAE/ZnO–Ag coating.

Conflicts of interest

There are no conflicts to declare.

Acknowledgements

The authors would like to thank Vietnam Academy of Science and Technology, for financial support (Grant # NCXS 01.01/22-24).

References

1 P. Nguyen-Tri, H. N. Tran, C. Ouellet Plamondon, L. Tuduri, D. V. N. Vo, S. Nanda, M. Abhilasha, H. P. Chao and A. K. Bajpai, Recent progress in the preparation, properties and applications of superhydrophobic nano-based coatings and surfaces: A review, *Prog. Org. Coat.*, 2019, **132**, 235–256.
2 T. V. Nguyen, T. P. Nguyen, T. D. Nguyen, R. Aidani, V. T. Trinh and C. Decker, Accelerated degradation of water borne acrylic nanocomposites used outdoor protective coatings, *Polym. Degrad. Stab.*, 2016, **128**, 65–76.
3 T. V. Nguyen, P. H. Dao, K. L. Duong, Q. H. Duong, Q. T. Vu, A. H. Nguyen, V. P. Mac and T. L. Le, Effect of R-TiO_2 and ZnO nanoparticles on the UV-shielding efficiency of water-borne acrylic coating, *Prog. Org. Coat.*, 2017, **110**, 114–121.
4 H. Salmi, X. Allonas and C. Ley, Polythiourethane networks catalyzed by photobase generators, *Prog. Org. Coat.*, 2016, **100**, 81–85.
5 F. Magnoni, A. Rannée, L. Marasinghe, B. El-Fouhaili, X. Allonas and C. Croutxé-Barghorn, Correlation between the scratch resistance of UV-cured PUA-based coatings and the structure and functionality of reactive diluents, *Prog. Org. Coat.*, 2018, **124**, 193–199.
6 E. Bakhshandeh, S. Bastani, M. R. Saeb, C. Croutxé-Barghorn and X. Allonas, High-performance water-based UV-curable soft systems with variable chain architecture for advanced coating applications, *Prog. Org. Coat.*, 2019, **130**, 99–113.
7 P. Nguyen-Tri and T. V. Nguyen, Radically curable nanobased coatings (chapter 10), in *Nanomaterials Based Coatings*, ed. P. Nguyen-Tri, S. Rtimi and C. Ouellet-Plamondon, Elsevier,

2019, pp. 1–35, ISBN: B978-0-12-815884-5.00001-6, DOI: 10.1016/B978-0-12-815884-5.00010-7.

8 T. V. Vu, V. T. Nguyen, P. Nguyen-Tri, T. H. Nguyen, T. V. Nguyen and T. A. Nguyen, Chapter 17 - Antibacterial nanocomposite coatings, *In Micro and Nano Technologies, Nanotoxicity*, ed. S. Rajendran, A. Mukherjee, T. A. Nguyen, C. Godugu and R. K. Shukla, Elsevier, 2020, pp. 355–364, ISBN 9780128199435, DOI: 10.1016/B978-0-12-819943-5.00017-8.

9 T. V. Nguyen, T. A. Nguyen, P. H. Dao, V. P. Mac, A. H. Nguyen, M. T. Do and T. H. Nguyen, Effect of rutile titania dioxide nanoparticles on the mechanical property, thermal stability, weathering resistance and antibacterial property of styrene acrylic polyurethane coating, *Adv. Nat. Sci.: Nanosci. Nanotechnol.*, 2016, **7**(4), 045015–045024.

10 A. M. El Saeed, M. A. El-Fattah and A. M. Azzam, Synthesis of ZnO nanoparticles and studying its influence on the antimicrobial, anticorrosion and mechanical behavior of polyurethane composite for surface coating, *Dyes Pigm.*, 2015, **121**, 282–289.

11 M. Akbarian, M. E. Olya, M. Ataeefard and M. Mahdavian, The influence of nanosilver on thermal and antibacterial properties of a 2 K waterborne polyurethane coating, *Prog. Org. Coat.*, 2012, **75**(4), 344–348.

12 R. D. Toker, N. Kayaman-Apohan and M. V. Kahraman, UV-curable nano-silver containing polyurethane based organic–inorganic hybrid coatings, *Prog. Org. Coat.*, 2013, **76**(9), 1243–1250.

13 T. T. Le, T. V. Nguyen, T. A. Nguyen, T. T. H. Nguyen, T. Hoang, D. L. Tran, D. A. Dinh, T. M. Nguyen and L. T. Lu, Thermal, mechanical and antibacterial properties of water-based acrylic polymer/SiO_2-Ag nanocomposite coating, *Mater. Chem. Phys.*, 2019, **232**, 362–366.

14 K. I. Dhanalekshmi, V. T. Nguyen and P. Magesan, Chapter 26 - Nanosilver loaded oxide nanoparticles for antibacterial application, *In Micro and Nano Technologies, Smart Nanocontainers*, ed. P. Nguyen-Tri, T.-O. Do and T. A. Nguyen, Elsevier, 2020, pp. 445–458, ISBN 9780128167700, DOI: 10.1016/B978-0-12-816770-0.00026-5.

15 P. Nguyen Tri, T. A. Nguyen, T. H. Nguyen and P. Carriere, Antibacterial Behavior of Hybrid Nanoparticles (Chapter 7), in *Noble Metal-Metal Oxide Hybrid Nanoparticles: Fundamentals and Applications*, ed. S. Mohapatra, T. A. Nguyen and P. Nguyen-Tri, 2019, pp. 141–155, DOI: 10.1016/B978-0-12-814134-2.00007-3.

16 T. D. Ngo, T. M. H. Le, T. H. Nguyen, T. V. Nguyen, T. A. Nguyen, T. L. Le, T. T. Nguyen, T. T. V. Tran, T. B. T. Le and N. H. Doan, Antibacterial nanocomposites based on Fe_3O_4-Ag hybrid nanoparticles and natural rubber–polyethylene blends, *Int. J. Polym. Sci.*, 2016, **2016**, 7478161.

17 T. N. L. Nguyen, T. V. Do, T. V. Nguyen, D. P. Hung, V. T. Trinh, V. P. Mac, A. H. Nguyen, D. A. Dinh, T. A. Nguyen, T. K. A. Vo, D. L. Tran and T. L. Le, Antimicrobial activity of acrylic polyurethane/Fe_3O_4-Ag nanocomposite coating, *Prog. Org. Coat.*, 2019, **132**, 15–20.

18 K.-H. Nam, K. Seo, J. Seo, S. B. Khan and H. Han, Ultraviolet-curable polyurethane acrylate nanocomposite coatings based on surface-modified calcium carbonate, *Prog. Org. Coat.*, 2015, **85**, 22–30.

19 C. E. Corcione, C. Ingrosso, F. Petronella, R. Comparelli and M. Lucia Curri, A designed UV–vis light curable coating nanocomposite based on colloidal TiO2 NRs in a hybrid resin for stone protection, *Prog. Org. Coat.*, 2018, **122**, 290–301.

20 D. Işın, N. Kayaman-Apohan and A. Güngör, Preparation and characterization of UV-curable epoxy/silica nanocomposite coatings, *Prog. Org. Coat.*, 2009, **65**(4), 477–483.

21 S. Zhang, A. Yu, X. Song and X. Liu, Synthesis and characterization of waterborne UV-curable polyurethane nanocomposites based on the macromonomer surface modification of colloidal silica, *Prog. Org. Coat.*, 2013, **76**(7–8), 1032–1039.

22 V. Maurin, C. Croutxé-Barghorn, X. Allonas, J. Brendlé, J. Bessières, A. Merlin and E. Masson, UV powder coatings containing synthetic Ag-beidellite for antibacterial properties, *Appl. Clay Sci.*, 2014, **96**, 73–80.

23 T. V. Nguyen, X. H. Le, P. H. Dao, C. Decker and T. P. Nguyen, Stability of acrylic polyurethane coatings under accelerated aging tests and natural outdoor exposure: The critical role of the used photo-stabilizers, *Prog. Org. Coat.*, 2018, **124**, 137–146.

24 X. Shi, T. A. Nguyen, Z. Suo, Y. Liu and R. Avci, Effect of Nanoparticles on the Anticorrosion and Mechanical Properties of Epoxy Coating, *Surf. Coat. Technol.*, 2009, **204**(3), 237–245.

25 O. Becker, R. Varley and G. Simon, Morphology, thermal relaxations and mechanical properties of layered silicate nanocomposites based upon high-functionality epoxy resins, *Polymer*, 2002, **43**(16), 4365–4373.

26 J. Zhou, X. Allonas and X. Liu, Fluorinated organozirconiums: Enhancement of overcoming oxygen inhibition in the UV-curing film, *Prog. Org. Coat.*, 2018, **120**, 228–233.

27 T. V. Vu, M. Tabish, S. Ibrahim, M. H. Pham Thi, T. H. Nguyen, C. B. Van, T. V. Nguyen, L. Pham Thi, T. A. Nguyen and G. Yasin, Water-based acrylic polymer/ZnO–Ag nanocomposite coating for antibacterial application, *Surf. Rev. Lett.*, 2022, DOI: 10.1142/S0218625X22501098.

28 V. T. Nguyen, V. T. Vu, T. H. Nguyen, T. A. Nguyen, V. K. Tran and P. Nguyen-Tri, Antibacterial Activity of TiO_2- and ZnO-Decorated with Silver Nanoparticles, *J. Compos. Sci.*, 2019, **3**, 61, DOI: 10.3390/jcs3020061.

29 Methods for Synthesis of Hybrid Nanoparticles, in *Noble Metal - Metal Oxide Hybrid Nanoparticles: Fundamentals and Application*, ed. S. Mohapatra, T. A. Nguyen and P. Nguyen-Tri, Elsevier, USA, 2018, ISBN: 978-0-12-814134-2, DOI: 10.1016/B978-0-12-814134-2.00003-6.

30 T. V. Nguyen, T. V. Do, M. H. Ha, H. K. Le, T. T. Le, T. N. L. Nguyen, X. T. Dam, L. T. Lu, D. L. Tran, Q. T. Vu, D. A. Dinh, T. C. Dang and P. Nguyen-Tri, Crosslinking

process, mechanical and antibacterial properties of UV-curable acrylate/Fe3O4-Ag nanocomposite coating, *Prog. Org. Coat.*, 2020, **139**, 105325.

31 M. M. Devi, S. H. Singh, K. Kaur, A. Gupta, A. Das, S. T. Nishanthi, C. Bera, A. K. Ganguli and M. Jha, New approach for the transformation of metallic waste into nanostructured Fe3O4 and SnO2-Fe3O4 heterostructure and their application in treatment of organic pollutant, *Waste Manag.*, 2019, **87**, 719–730, DOI: **10.1016/j.wasman.2019.03.007**.

32 P. Kaali, E. Strömberg, R. E. Aune, G. Czél, D. Momcilovic and S. Karlsson, Antimicrobial properties of Ag+ loaded zeolite polyester polyurethane and silicone rubber and long-term properties after exposure to *in vitro* ageing, *Polym. Degrad. Stab.*, 2010, **95**(Issue 9), 1456–1465.

33 C. Damm, H. Münstedt and A. Rösch, The antimicrobial efficacy of polyamide 6/silver-nano- and microcomposites, *Mater. Chem. Phys.*, 2008, **108**(Issue 1), 61–66.

34 M. Raula, M. H. Rashid, T. K. Paira, E. Dinda and T. K. Mandal, Ascorbate-Assisted Growth of Hierarchical ZnO Nanostructures: Sphere, Spindle, and Flower and Their Catalytic Properties, *Langmuir*, 2010, **26**(11), 8769–8782.

35 H. R. Liu, G. X. Shao, J. F. Zhao, Z. X. Zhang, Y. Zhang, J. Liang, X. G. Liu, H. S. Jia and B. S. Xu, Worm-Like Ag/ZnO Core–Shell Heterostructural Composites: Fabrication, Characterization, and Photocatalysis, *J. Phys. Chem. C*, 2012, **116**(30), 16182–16190, DOI: **10.1021/jp2115143**.

36 P. Nguyen Tri, S. Rtimi, T. A. Nguyen and M. T. Vu, Chapter 5 - Physics, Electrochemistry, Photochemistry, and Photoelectrochemistry of Hybrid Nanoparticles, *In Micro and Nano Technologies, Noble Metal-Metal Oxide Hybrid Nanoparticles*, ed. S. Mohapatra, T. A. Nguyen and P. Nguyen-Tri, Woodhead Publishing, 2019, pp. 95–123, ISBN 9780128141342, DOI: **10.1016/B978-0-12-814134-2.00005-X**.

37 F. Li, Y. L. Yuan, J. Y. Luo, Q. H. Qin, J. F. Wu, Z. Li and X. T. Huang, Synthesis and characterization of ZnO–Ag core–shell nanocomposites with uniform thin silver layers, *Appl. Surf. Sci.*, 2010, **256**, 6076–6082.

38 Y. C. Lu, Y. H. Lin, D. J. Wang, L. L. Wang, T. F. Xie and T. F. J. Jiang, Surface charge transfer properties of high-performance Ag-decorated ZnO photocatalysts, *J. Phys. D: Appl. Phys.*, 2011, **44**, 315502.

39 *Noble Metal-Metal Oxide Hybrid Nanoparticles: Fundamentals and Applications*, ed. S. Mohapatra, T. A. Nguyen and P. Nguyen-Tri, Elsevier, 2019, DOI: **10.1016/C2017-0-00847-9**.

40 T. V. Nguyen, P. Nguyen-Tri, S. Azizi, T. C. Dang, D. M. Hoang, T. H. Hoang, T. L. Nguyen, T. T. L. Bui, V. H. Dang, N. L. Nguyen, T. T. Le, T. N. L. Nguyen, Q. T. Vu, D. L. Tran, T. M. L. Dang and L. T. Lu, The role of organic and inorganic UV-absorbents on photopolymerization and mechanical properties of acrylate-urethane coating, *Mater. Today Commun.*, 2020, **22**, 100780, DOI: **10.1016/j.mtcomm.2019.100780**.

41 N. L. Nguyen, T. M. L. Dang, T. A. Nguyen, H. T. Ha and T. V. Nguyen, Study on Microstructure and Properties of the UV Curing Acrylic Epoxy/SiO2 Nanocomposite Coating, *J. Nanomater.*, 2021, **2021**, 8493201, DOI: **10.1155/2021/8493201**.

42 R. Fouladi-Fard, R. Aali, S. Mohammadi-Aghdam and S. Mortazavi-derazkola, The surface modification of spherical ZnO with Ag nanoparticles: A novel agent, biogenic synthesis, catalytic and antibacterial activities, *Arabian J. Chem.*, 2022, **15**(3), 103658, DOI: **10.1016/j.arabjc.2021.103658**.

43 J. G. Cuadra, L. Scalschi, B. Vicedo, M. Guc, V. Izquierdo-Roca, S. Porcar, D. Fraga and J. B. Carda, ZnO/Ag Nanocomposites with Enhanced Antimicrobial Activity, *Appl. Sci.*, 2022, **12**, 5023, DOI: **10.3390/app12105023**.